

HYDROGEN SELF-IGNITION IN PRESSURE RELIEF DEVICES

Golub, V.V., Semin, N.V., Laskin I.N., Lenkevich, D.A. and Volodin, V.V.
Department of Physical Gasdynamics, Joint Institute for High Temperatures, Izhorskaya str.
13/19, 125412, Moscow, Russia, golub@ihed.ras.ru

ABSTRACT

In future pressure relief devices (PRDs) should be installed on hydrogen vehicles to prevent a hydrogen container burst in the event of a nearby fire. Weakening of the container at elevated temperature could result in such burst. In this case the role of a PRD is to release some or all of the system fluid in the event of an abnormally high pressure. The paper analyzes the possibility of hydrogen self-ignition at PRD operation and ways of its prevention.

1.0 INTRODUCTION

Motivation for safety investigation of hydrogen arises from the global trend to find alternative energy sources as a replacement for conventional fuels. In several fields, for instance chemical industry, hydrogen has been safely produced, distributed, and used for many decades. However, the developed safety procedures and technologies provide only limited guidance for future stationary and mobile hydrogen applications. Namely, in the case of hydrogen powered vehicles, hydrogen will be utilized within a decentralized infrastructure in relatively small amounts (several kg per user) by a large population without special training in the safety of combustible gases [1]. The public will accept future hydrogen technologies only if a safety level comparable to that of current technologies can be obtained.

In the review by Astbury and Hawksworth [2] a rigorous research was done on accidents involving spontaneous ignition of hydrogen at high pressure. Over the last century, 81 major accidents were reported. It turned out that in 86% of cases there was no clearly identifiable ignition source. Several mechanisms have been postulated as responsible ones for this phenomenon, for example, reverse Joule-Tompson effect, electrostatic ignition, and sudden adiabatic compression. However, none of these causes could stand up detailed scientific analysis except one. In 1973, Wolański and Wójcicki observed that hydrogen heated below the auto-ignition threshold could ignite if it was released into an open space with oxygen or air. They suggested that ignition occurred due to high jump in temperature on the contact surface, where heated by a primary shock wave oxygen mixed and reacted with hydrogen due to diffusion. Thus, for the first time, diffusion self-ignition mechanism was proposed [3]. Recently, this scenario attracted lots of interests as a possible cause for industrial hazards [4-12].

Unlike in the experiment conducted by Wolański and Wójcicki, Baev [4] poured hydrogen into a partly closed tube preliminary heating it. However, the tube had several obstacles, and hydrogen self-ignition was observed only after a shock wave reflected from the obstacles. In the investigation by Mogi [5] ruptured disk was used in the rapid discharge of high-pressure hydrogen into a tube 5-10 mm in diameter with an open end. The failure pressure was changed from 40 to 400 bar. Ignition of the hydrogen jet was observed in the extension tube. The paper of Dryer [6] reports the similar mechanism of hydrogen and natural gas self-ignition at the burst disk failure and combustible gas release into the tube filled with air. Furthermore, the transverse shocks formed the burst disk failure led to heating of the gas on the contact surface. In work by Golub [7] the self-ignition of high-pressure hydrogen in tubes of round and rectangular cross sections is investigated experimentally and numerically. Mechanisms leading to hydrogen self-ignition in a tube have been determined.

Previously, most of works devoted to hydrogen safety investigated discharge into tubes or confined space. The aim of this investigation is a numerical study of boundary phenomena influence on the hydrogen self-ignition at the discharge into the semi-confined space

Xu et al [9], Lui et al [10-11], used multi-component approach as well as ultra fine meshes for accurate calculation of molecular transport to investigate spontaneous ignition of pressurized hydrogen release through a tube into air. The study confirmed possibility of spontaneous ignition via molecular diffusion.

2.0 NEW CONCEPT FOR PRESSURE RELEASE VALVE NOZZLE DESIGN

Previously, most of works devoted to hydrogen safety investigated discharge into tubes or confined space. The aim of this investigation is a numerical and experimental study of boundary phenomena influence on the hydrogen self-ignition at the discharge into the semi-confined space.

In paper [12], numerical modeling of hydrogen jet has been conducted where hydrogen jetted into atmosphere through a symmetrical orifice in 2D case. Dependence of flame occurrence on orifice diameter has been obtained. It turned out that for diameter smaller than 2.6 mm the ignition did not started or died out fast, hydrogen pressure being up to 400 atm.

Based on the result of this work, an idea to replace a big release valve nozzle by several smaller nozzles of the same total area emerged. Consequently, in case of accidental high pressure hydrogen release there is a hope the ignition will not occur if boundary condition has been properly set. Namely, the diameter of the small orifices and the distance between them are matched in a way that every small orifice behaves like an isolated one, so that the ignition is inhibited due to rarefaction waves.

2.1 Numerical modeling of hydrogen jetted into atmosphere

Investigation of hydrogen jetting into the semi-confined space from a high pressure vessel was simulated numerically in the axisymmetrical two-dimensional (2D) case and in the three-dimensional (3D) case. Different geometries of technical openings have been studied, but overall area of the openings was the same in all cases. In particular, we have compared hydrogen release from one orifice of 4 mm in diameter and a system of 4 identical orifices with the diameter of 2 mm each (Figure 1). The total area was $16\pi \text{ mm}^2$ in both cases. The system of 4 identical orifices represented 4 circular holes, placed in the vertices of a square. The length of the square side – L – was a varying parameter in the calculations.

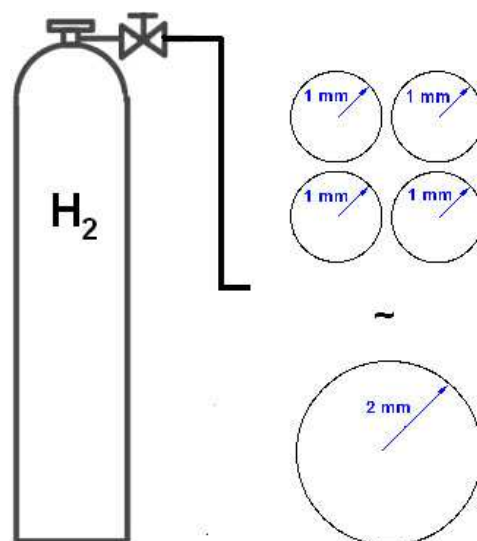


Figure 1. Different geometries of technical openings under investigation, but overall area of the openings was the same in all cases. Namely, one orifice of 2 mm in radius and a system of 4 identical orifices with the radius of 1 mm each

The numerical modeling of hydrogen jet self-ignition was performed based on the full system of Navier-Stokes equations for the multicomponent mixture of gases [13]. Chemical model in use involved the gas-dynamic transport of a viscous gas and the detailed kinetics of hydrogen oxidation [15-16]. Equations were solved with the upwind, finite volume procedure. The Roe flux vector-splitting scheme with a min mod limiter was used for the discretization of the fluxes in the equations. In the all cases considered here, the solid surface was assumed non-catalytic and adiabatic. The time step was $0.1 - 1 \mu\text{s}$.

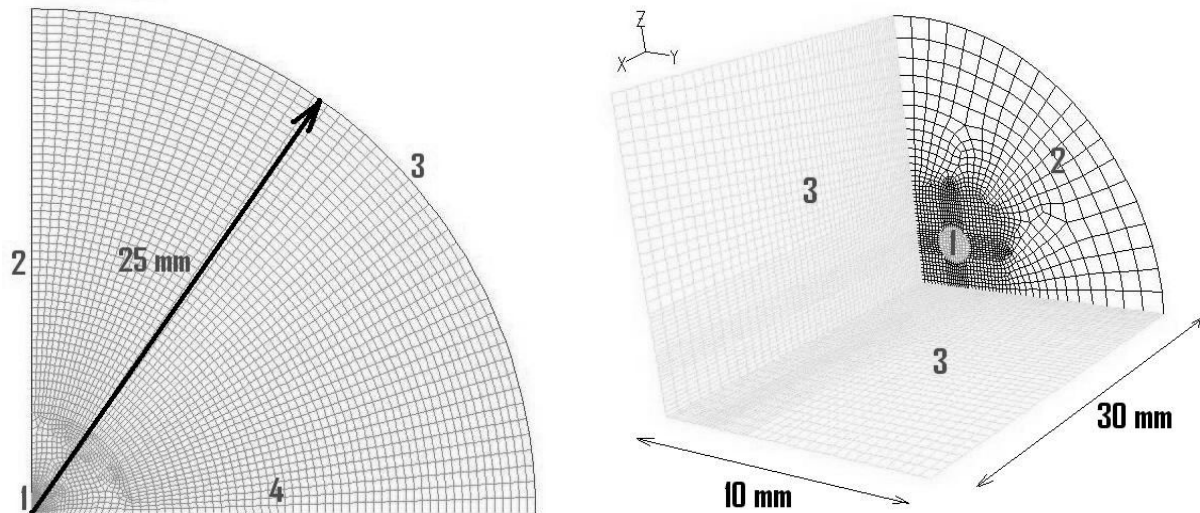


Figure 2. Computational grid in 2D (left) and 3D (right) cases. 2D (left): 1 – pressure inlet, 2 – wall, 3 – pressure outlet, 4 – symmetry axis. 3D (right): 1 – pressure inlet, 2 – wall, 3 – symmetry plane.

In 2D case computational domain represented a quarter of a circle of the radius 20-50 mm. Number of cells was $N = 100 \times 100$. Minimum space step was $0.1 \times 0.1 \text{ mm}^2$, maximum - $0.3 \times 0.3 \text{ mm}^2$. Boundary conditions are shown in Figure 2 (left).

In 3D case computational domain represented a quarter of a cylinder. The radius was 10-15 mm, the generatrix was 20-30 mm. Number of cells was $N = 50 \times 50 \times 100$. Minimum space step was $0.1 \times 0.1 \times 0.1 \text{ mm}^3$, maximum - $0.5 \times 0.5 \times 0.7 \text{ mm}^3$. Boundary conditions are shown in Figure 2 (right).

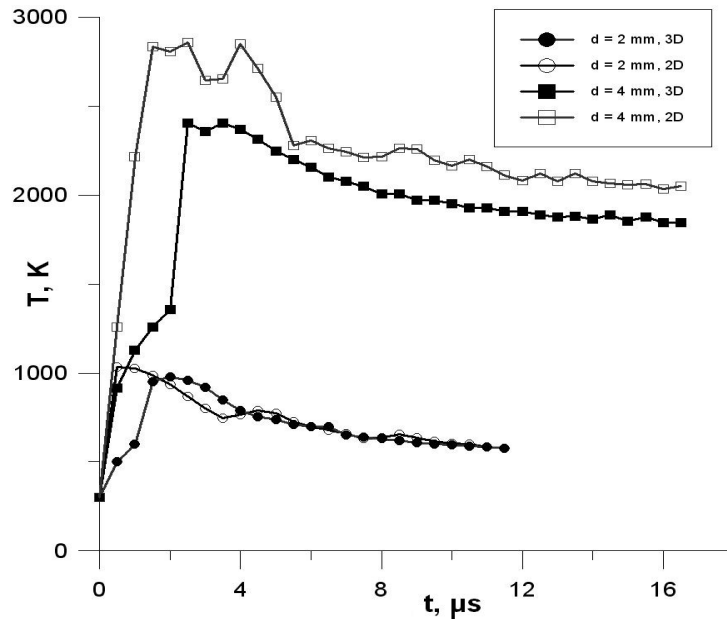


Figure 3. Maximum jet temperature vs. time. Initial pressure was 400 atm. Circles – orifice of 2 mm in diameter. Quads – 4 mm in diameter. Empty quads and circle correspond to calculations in 2D case, filled ones - 3D case.

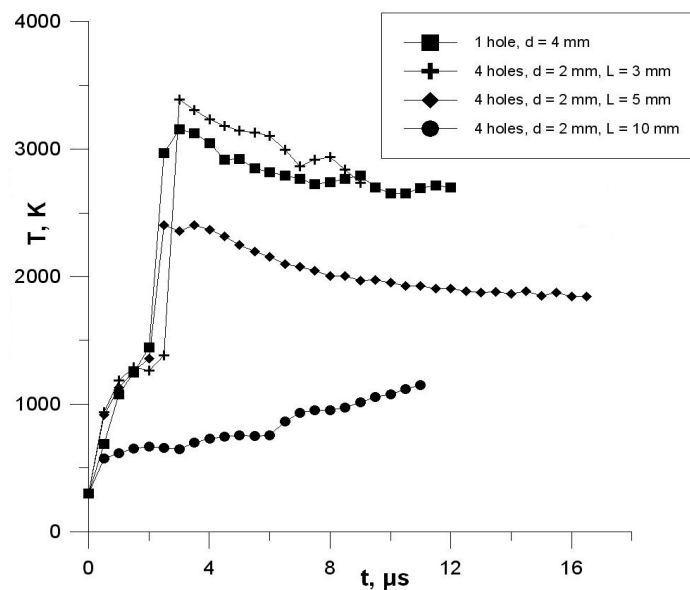


Figure 4. Maximum jet temperature vs. time. Initial pressure was 400 atm. Quads – 1 hole, $D = 4 \text{ mm}$. Crosses – 4 holes, $d = 2 \text{ mm}$, $L = 3 \text{ mm}$. Rhombuses – 4 holes, $d = 2 \text{ mm}$, $L = 5 \text{ mm}$. Circles – 4 holes, $d = 2 \text{ mm}$, $L = 10 \text{ mm}$.

At first, test calculations were done for a single orifice of diameter 2 mm and 4 mm in 3D case. Initial pressure was 400 atm. The results were correlated with the data from 2D calculations, and with results from the work [9]. The reason to do the test calculations was to make sure that the use of a rather coarse grid in 3D would not result in big numerical error. In Figure 3 a comparison in maximum temperature of the hydrogen jet between 2D and 3D cases for two different types of orifices is presented. Circles correspond to the orifice of 2 mm in diameter: empty circles – 2D case, filled circles – 3D case. Quads depict results for the orifice of 4 mm in diameter: empty quads – 2D case, filled

quads – 3D case. Test investigation did not reveal any significant difference in the data obtained after $2 \mu\text{s}$, the error being of the order of 10%. What was important that the general trend in temperature dependencies for the 3D case was conserved. Namely, ignition does occur for the orifice diameter 4 mm, but there is no ignition for the 2 mm orifice.

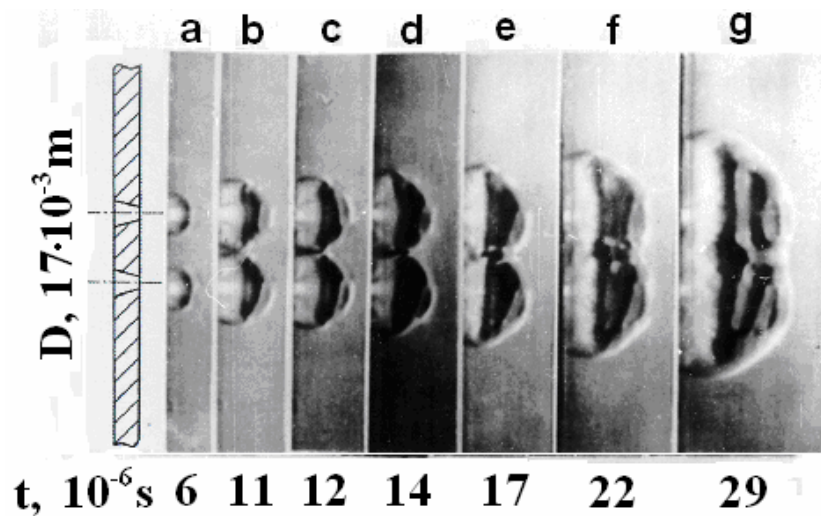


Figure 5. Toeplerograms of a nitrogen supersonic jet release into air.

Finally, simulations were performed to reveal influence of the distance between orifices on diffusion self-ignition. After replacement of the orifice with 4 mm diameter by area-equivalent system of 4 orifices with 2 mm diameter each, placed at 3 mm from each other, an increase in maximum jet temperature occurred (Figure 4, crosses plot). The explanation is the interference of shock waves on the axis of symmetry. In Figure 5 visualization performed by the schlieren method of exhaust from neighbouring nozzles is presented. It clearly shows that forming regular Mach reflection regime behind heading shockwaves leads to an increase in local temperature. However, when the distance between orifices got long enough in comparison with the diameter – 10 mm, the orifices behaved like independent ones, and the self-ignition did not occur (Figure 4, circles plot).

3.0 EXPERIMENTAL INVESTIGATION OF HYDROGEN SELF-IGNITION IN A PRESSURE RELIEF DEVICE

A Pressure Relief Device (PRD) is a safety device that is used to prevent a failure of the containment system by releasing some or all of the gaseous or liquid contents fast enough. Invented in the 17th century, PRDs became widespread in the early 1900s. A large chemical plant can have 500-10,000 PRDs [17]. The number of PRDs could dramatically increase with the development of hydrogen vehicles.

In Figure 6 a PRD from SHERWOOD Company is presented. This study revealed possible weakness of such device, if it is utilized in high pressure reservoirs with hydrogen. The study was undertaken with the help of the experimental setup, shown schematically in Figure 7. It consisted of a hydrogen cylinder (1) equipped with a valve (2) and a manometer (4) for measuring the pressure in the high-pressure hydrogen chamber (3). After pressure reached a particular value, hydrogen was released through a model of a PRD (T-mixer) (5). The hydrogen self-ignition was registered with the help of a photo-transducer (6).

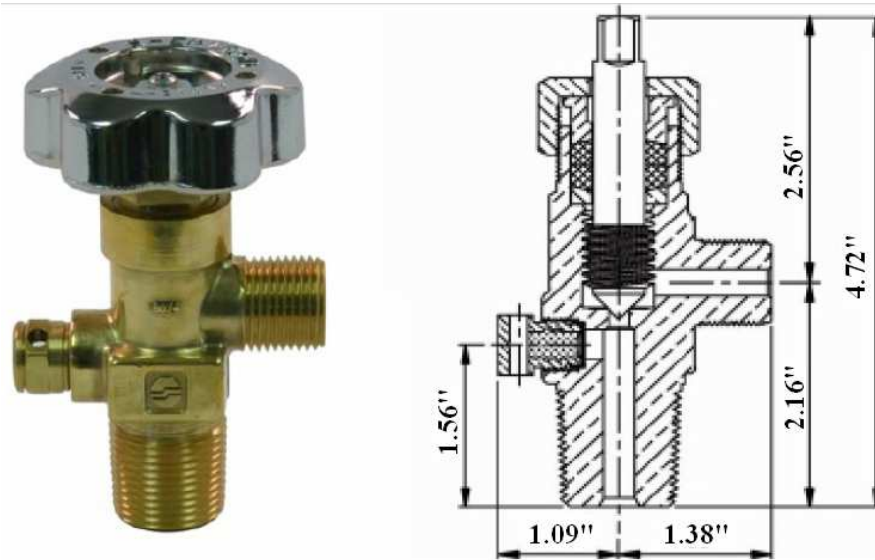


Figure 6. Photo of PRD valve from SHERWOOD Company (left), scheme of PRD valve (right).

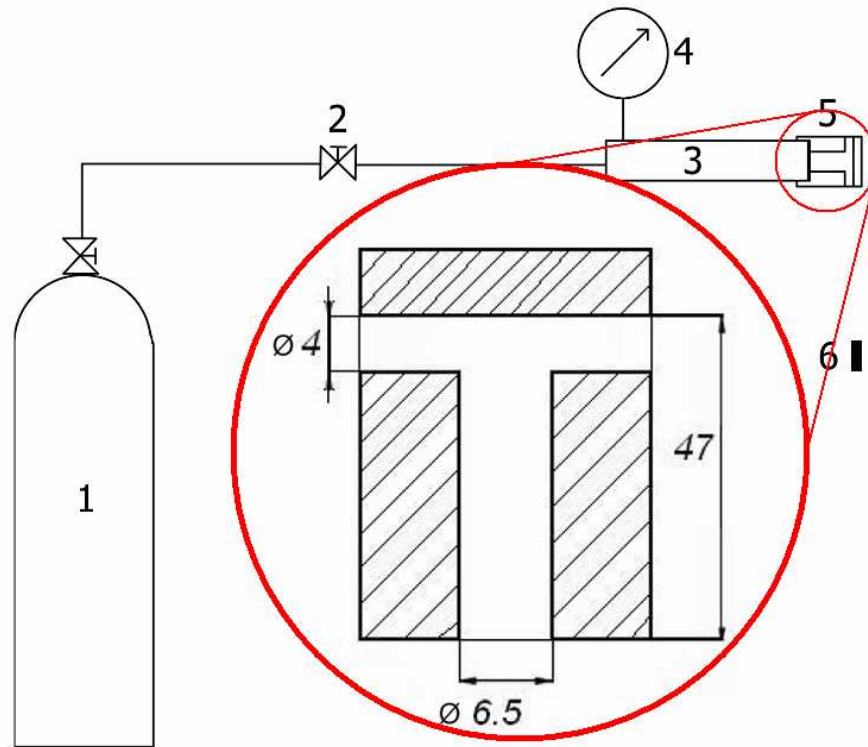


Figure 7. Schematic of the experimental set-up. 1 – hydrogen cylinder, 2 – valve, 3 – high pressure chamber, 4 – manometer, 5 – a model of PRD (T-mixer), 6 – photo-transducer.

Data in Table 1 shows that ignition in PRD-block is possible after the bust disk (BD) opening at the initial pressure of 37 bar. Also there is an overlap of pressure values that lead to ignition and the values that correspond to no ignition. Possibly it happens due to differences in BD opening [14].

Table 1. The data obtained in PRD-model from Figure 6.

Pressure, bar	36.8	44.8	52	53.6	57.6	58.4	61
Ignition	YES	NO	NO	YES	YES	NO	YES

4.0 NUMERICAL MODELING OF HYDROGEN SELF-IGNITION IN A X-MIXTURE CHANNEL

Experiments from the previous part indicated that some modification to PRD should be implemented to help inhibit self-ignition more successfully and reliably. The goal is to propose modifications to a conventional PDR model, to make sure that self-ignition does not take place if the pressure in the containment is below some reasonably high value. Experimental and numerical studies on the hydrogen self-ignition phenomena indicate that increasing outflow from stagnation zone (tube bends) will result in temperature drop, thus conditions for the self-ignition to occur become less favorable [1-14]. For this purpose numerical simulations were, trying to compare flow in T- and X-mixers.

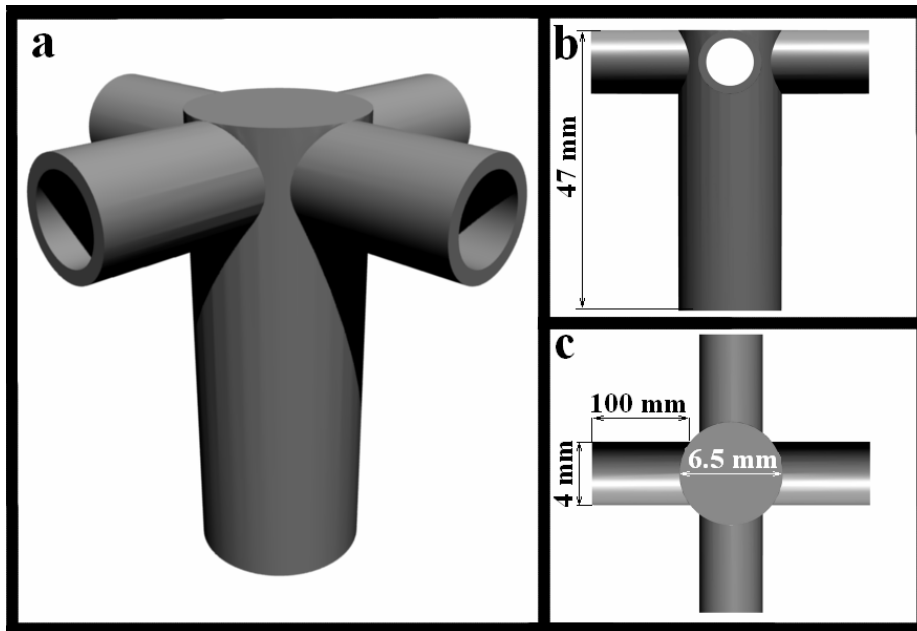


Figure 8. X-mixer geometry: a – 3d view, b – front view, c – top view. The tube diameter was 6.5 mm, length – 47 mm; the pipe bends diameter was 4 mm, length – 100 mm.

Computational domain represented a main tube and X pipe bends (Figure). The tube diameter was 6.5 mm, length – 47 mm; the pipe bends diameter was 4 mm, length – 100 mm. Initial conditions at the main tube inlet were: mass fraction of oxygen 0.23, mass fraction of nitrogen 0.77, pressure $P = 1$ atm, temperature $T = 300$ K. High pressure chamber initial conditions were: mass fraction of hydrogen 1, mass fraction of oxygen 0, pressure $P = 20 - 100$ atm, temperature $T = 300$ K.

Boundary conditions for wall implied non-catalytic surfaces and no slip condition. The bottom part of the computational domain was a pressure inlet for impulse hydrogen jet. The top part was a wall. Influence of the boundary layer was neglected.

The temperature of mixture higher than 1500 K with the appearance of a H_2O mass fraction $\sim 10^{-4}$ was assumed as the criterion of the hydrogen ignition. Significant increase in concentration of H_2O and

further increase in temperature up to 2000 – 3000 K indicated on self-sustenance of combustion process.

The computational grid had 60x60x200 mesh points for the main tube and 60x60x100 for X pipe bends. The time step was 1-1.5 μ s.

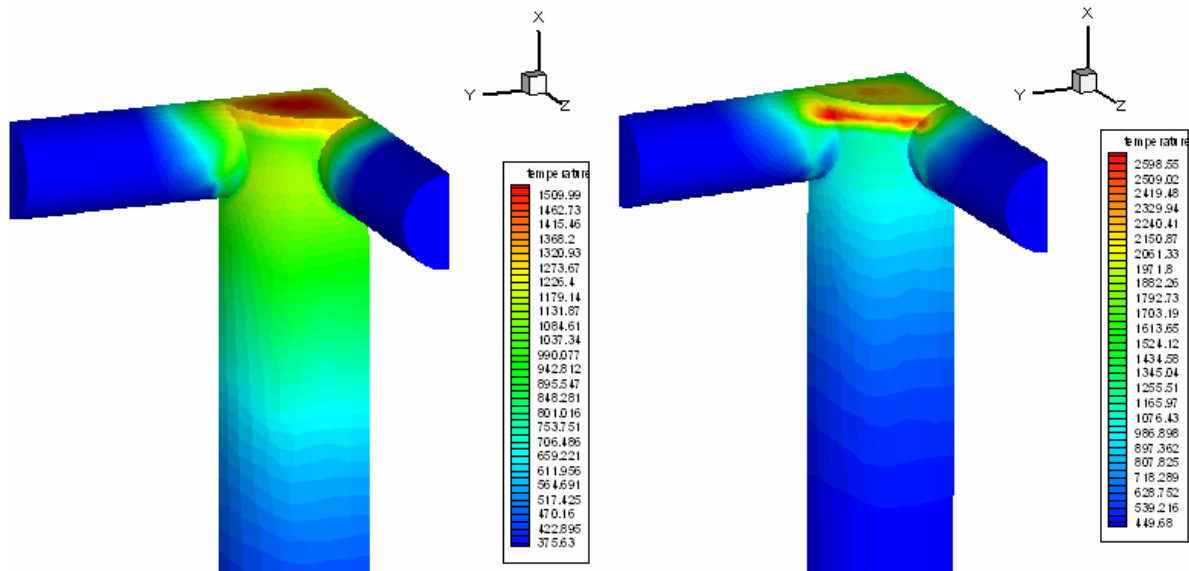


Figure 9. Temperature distribution at 2 different time moments for the X-channel. Due to symmetry, only quarter of the geometry is shown. Left: $t = 3 \cdot 10^{-5}$ s – no combustion. Right: $t = 3.1 \cdot 10^{-5}$ s – combustion started.

In calculations development of flow in X-channel was obtained. In Figure 9 distribution of temperature on walls at different time moments is presented. Due to symmetry, only quarter of the geometry is shown. Initial pressure at the pressure inlet was 26 atm. At time $t = 3 \cdot 10^{-5}$ maximum temperature was about 1600 K. At time $t = 3.1 \cdot 10^{-5}$ self-ignition takes place, that leads to combustion. Maximum temperature grows up to 2000 K.

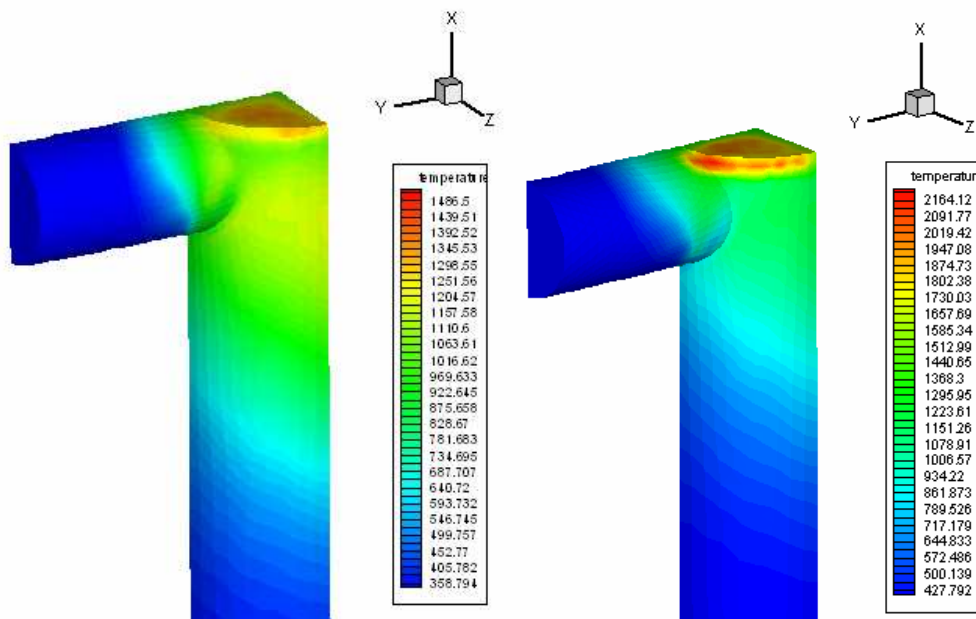


Figure 10. Temperature distribution at 2 different time moments for the T-channel. Due to symmetry, only quarter of the geometry is shown. Left: $t = 2.9 \cdot 10^{-5}$ s – no combustion. Right: $t = 3 \cdot 10^{-5}$ s – combustion started.

In Figure 10 analogous distribution of temperature for the case T-channel is presented. Due to symmetry, only quarter of the geometry is shown. Initial pressure at the pressure inlet was 26 atm. In this case ignition takes places somewhat earlier at $t = 2.9 \cdot 10^{-5}$.

Finally, comparison in H₂O mass concentration for the T-channel and the X-channel at the same time moment is depicted in Figure 11. Due to symmetry, only half of the geometry is shown. The process of self-ignition and further combustion is clearly seen from left Figure 8 for the T-channel, meanwhile there is no apparent sign of the process in right Figure 11 for the X-channel.

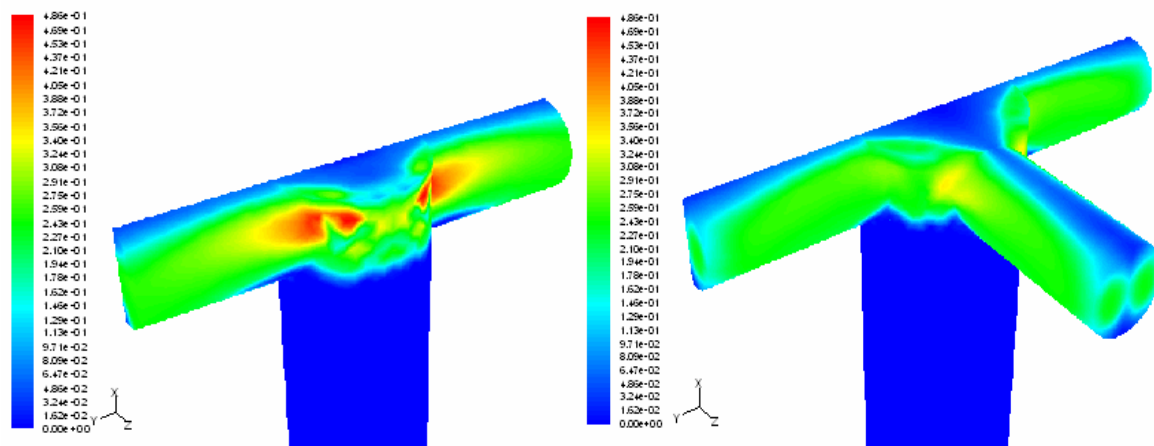


Figure 11. H₂O mass concentration at the same time moment $t = 2.9 \cdot 10^{-5}$ s for the T-channel (left) and the X-channel (right). . Due to symmetry, only half of the geometry is shown.

5.0 CONCLUSION

In this work, an investigation of hydrogen jet at its release into atmosphere from a high pressure vessel was done. Results for several boundary and initial conditions have been compared. It was obtained that after replacement of the orifice with 4 mm diameter by area-equivalent system of 4 orifices with 2 mm diameter each, placed at 10 mm from each other, diffusion self-ignition was successfully depressed.

It was shown experimentally that at the initial pressure of 37 bar and higher hydrogen self-ignition discharge in a PRD-model is possible.

Numerical modeling demonstrated that utilization of an X-mixture channel in PRDs could inhibit hydrogen self-ignition more successfully than original design of PRD. New standards in PRDs are needed nowadays.

REFERENCES

1. Breitung, W., Mechanistic safety analysis of hydrogen based energy systems, Proceedings of the 2nd European Summer School on Hydrogen Safety, 30 July - 8 August, Belfast, 2007, Keynote Lectures, 2.

2. Astbury, G.R., Hawksworth, S.J., Spontaneous ignition of hydrogen leaks: A review of postulated mechanisms, *International Journal of Hydrogen Energy*, **32**, 2007, N. 13, pp. 2178-2185.
3. Wola'nski, P., W'ojcicki, S., Investigation into the mechanics of the diffusion ignition of a combustible gas flowing into an oxidizing atmosphere, Proceedings of the 14th International Symposium on Combustion, pp. 1217 - 1223.
4. Baev, V.K., Buzukov, A.A., Shumskii, V.V., Conditions of selfignition at impulse high pressure injection of combustible gases in confined volume, *Combustion and Explosion*, **36**, 2000, N. 3, pp. 3-9.
5. Mogi, T., Shiina, H., Kim, D., Horigushi, S., Ignition of high pressure hydrogen by a rapid discharge, Proceedings of the 31st International Symposium on Combustion, 6 – 11 August, Heilderberg, 2006, Germany.
6. Dryer, F., Chaos, M., Zhao, Zh., Stein, J., Alpert, J., Homer, Ch., Spontaneous ignition of pressurized release of hydrogen and natural gas into air, *Combustion Science and Technology*, **179**, 2007, pp. 663-694.
7. Golub, V.V., Baklanov, D.I., Bazhenova, T.V., Bragin, M.V., Golovastov, S.V., Ivanov, M.F., Volodin, V.V. Shock-induced ignition of hydrogen gas during accidental or technical opening of high-pressure tanks, *Journal of Loss Prevention in the Process Industries*, **20**, 2007, N. 4-6. pp. 439-446..
8. Mogi, T., Kim, D., Shiina, H., Sadashige, H., Self-ignition and explosion during discharge of high-pressure hydrogen, *Journal of Loss Prevention in the Process Industries*, **21**, 2008, pp. 199-204.
9. Xu, B.P., Hima, L.El., Wen, J.X., Dembele, S., Tam, V.H.Y., Donchev, T., Numerical study on the spontaneous ignition of pressurized hydrogen release through a tube into air. *Journal of Loss Prevention in the Process Industries*, **21**, 2008, pp. 205-213.
10. Liu, Y.F., Sato, H., Tsuboi, N., Njigashino, F., Hayashi, A.K., Direct numerical simulation on hydrogen fuel jetting from high pressure tank, Proceedings of the 20th International Colloquium on the Dynamics of Explosions and Reactive Systems (ICDERS), 2005, Montreal, Canada.
11. Liu, Y.F., Sato, H., Tsuboi, N., Njigashino, F., Hayashi, A.K., Numerical simulation on hydrogen fuel jetting from high pressure tank, *Science Tech Energy Mater*, **67**, pp. 7-11.
12. Bazhenova, T.V., Bragin, M.V., Golub, V.V., Ivanov, M.F., Self-ignition of a fuel gas upon pulsed efflux into an oxidative medium, *Technical Physics Letters*, **32**(3), 2006, pp. 269-271
13. Baev, V., Golovitchev, V., Tretjakov, P., and et al., Combustion in Supersonic Flow, NASA TM-77822, March 1985.
14. Xu, B.P., Wen, J.X., Dembele, S., Tam, V.H.Y, Hawksworth, S.J., The effect of pressure boundary rupture rate on spontaneous ignition of pressurized hydrogen release, *Journal of Loss Prevention in the Process Industries*, **22**(3), 2009, pp. 279-287
15. Miller, J.A., Bowman, C.I., Mechanism and Modeling of Nitrogen Chemistry in Combustion, *Progress in Energy Combust. Sci.* 1989. V.15.
16. Miller J.A., Kee R.J., Rupley F.M. "CHEMKIN-II: A Fortran Chemical Kinetics Package for the Analysis of Gas Phase Chemical Kinetics", Sandia National Laboratories Technical Rep. SAND86-8009B/UC-706, 1991
17. Sunderland P.B., Pressure relief devices for hydrogen vehicles, Teaching Materials of the 3rd European Summer School on Hydrogen Safety.
<http://www.engi.ulst.ac.uk/esshs/php/ESSHSTeachingMaterials.php>

APPENDIX A

The numerical modeling of the self-ignition of a hydrogen jet was performed based on the full system of Navier-Stokes equations for the multicomponent mixture of gases:

$$\frac{\partial \vec{q}}{\partial t} + \frac{\partial \vec{E}}{\partial x} + \frac{\partial (\vec{F} + \vec{F}_v)}{\partial y} = 0, \quad (1)$$

vectors \vec{E}, \vec{F} correspond to the Euler equations, vector \vec{F}_v correspond to the viscous stresses:

$$\vec{q} = \begin{pmatrix} \rho \\ \rho u \\ \rho v \\ \rho e \\ \rho c_k \end{pmatrix}; \quad \vec{E} = \begin{pmatrix} \rho u \\ \rho u^2 + p \\ \rho uv \\ \rho u(h + V^2/2) \\ \rho u c_k \end{pmatrix}; \quad \vec{F} = \begin{pmatrix} \rho v \\ \rho uv \\ \rho v^2 + p \\ \rho v(h + V^2/2) \\ \rho v c_k \end{pmatrix}; \quad \vec{F}_v = \begin{pmatrix} 0 \\ \sigma_{yx} \\ \sigma_{yy} \\ q_y \\ J_k^y \end{pmatrix}; \quad (2)$$

where u, v - cartesian components of velocity vector, $V = \sqrt{u^2 + v^2}$ - velocity ρ - density, p - pressure, e - total energy, h - the specific enthalpy of mixture, c_k - mass fraction of the k component:

$$\begin{aligned} \sigma_{yx} &= -(\mu) \frac{\partial u}{\partial y} \\ \sigma_{yy} &= -\frac{4}{3}(\mu) \frac{\partial v}{\partial y} \\ q_y &= u \sigma_{yx} + v \sigma_{yy} - \left(\frac{\mu}{Pr} \right) \frac{\partial h}{\partial y} + \\ &\quad + \frac{\mu}{Pr} \sum_k (Le_k - 1) h_k \frac{\partial c_k}{\partial y} \\ J_k^y &= -\left(\frac{\mu}{Pr} Le_k \right) \frac{\partial c_k}{\partial y} \end{aligned} \quad (3)$$

Here $Pr=0.72$ - molecular Prandtl number, $Le_k=1$ - molecular Lewis number of k component, μ - coefficient of dynamic viscosity. Calculations were performed in the laminar approach.

The subsystem of the transport equations for the component of the mixture of system (1), introduced to account for the high-constituent nature of medium and of chemical kinetics:

$$\begin{aligned} \frac{\partial}{\partial t}(\rho c_k) + \frac{\partial}{\partial x}(\rho c_k u) + \frac{\partial}{\partial y}(\rho c_k v) + j \frac{\rho c_k v}{y} = \\ = \frac{\partial}{\partial x} \left[\left(\frac{\mu}{Sc_k} \right) \frac{\partial c_k}{\partial x} \right] + \frac{\partial}{\partial y} \left[\left(\frac{\mu}{Sc_k} \right) \frac{\partial c_k}{\partial y} \right] + \omega_k \end{aligned} \quad (4)$$

Here ω_k - chemical source, and $Sc_k = \mu / \rho D_k$, where D_k - diffusion coefficient. The influence of chemical reactions to the flow of gas appears as source term in the right sides of the transport equation. According to the law of mass action the expression for the source term is written in the following form:

$$\omega_k = \mu_k \sum_{l=1}^{m_r} \Delta v_{kl} r_l = \mu_k \sum_{l=1}^{m_r} (v'_{kl} - v_{kl}) r_l ; k=1,2,\dots,K,$$

$$r_l = k_{+l} \rho^{v_l} \prod_{j=1}^K \left(\frac{c_j}{\mu_j} \right)^{v_{jl}} - k_{-l} \rho^{v'_l} \prod_{j=1}^K \left(\frac{c_j}{\mu_j} \right)^{v'_{jl}},$$

$$\text{and } v_l = \sum_{j=1}^K v_{jl} ; v'_l = \sum_{j=1}^K v'_{jl}.$$

Here μ_i , v_{il} , v'_{il} , k_{+l} , k_{-l} , K , m_r - the molecular weight of the I component, stoichiometric coefficients and the rate constant of forward and backward reactions, the number of components and reactions respectively. The constants of reactions are written in the Arrhenius form:

$$k_{\pm l} = A_{\pm l} T^{n_{\pm l}} \exp(-E_{\pm l} / RT),$$

where $A_{\pm l}$, $n_{\pm l}$, $E_{\pm l}$ are constants.

Physicochemical properties are supposed to be functions of the local mixture composition, temperature and pressure. They are computed using the CHEMKIN-II subroutines.

The chemical kinetics mechanism for the hydrogen oxidation is due to Bowman and Miller (1989). This mechanism considers 11 species H₂O, O₂, H₂, OH, H, O, HO₂, H₂O₂, N₂, NO, N (M – third particle) and 21 elementary reactions:

- 1) H₂O + M = H + OH + M
- 2) H₂ + M = H + H + M
- 3) O₂ + M = O + O + M
- 4) H + O + M = OH + M
- 5) O + H₂ = OH + H
- 6) O₂ + H = O + OH
- 7) O + H₂O = OH + OH
- 8) H₂O + H = OH + H₂
- 9) H₂ + O₂ = OH + OH
- 10) H₂O₂ + M = OH + OH + M
- 11) HO₂ + M = H + O₂ + M
- 12) HO₂ + H₂ = H₂O₂ + H

- 13) $\text{H}_2\text{O} + \text{HO}_2 = \text{H}_2\text{O}_2 + \text{OH}$
- 14) $\text{H} + \text{HO}_2 = \text{OH} + \text{OH}$
- 15) $\text{O} + \text{HO}_2 = \text{O}_2 + \text{OH}$
- 16) $\text{OH} + \text{HO}_2 = \text{H}_2\text{O} + \text{O}_2$
- 17) $\text{HO}_2 + \text{HO}_2 = \text{H}_2\text{O}_2 + \text{O}_2$
- 18) $\text{H} + \text{HO}_2 = \text{H}_2 + \text{O}_2$
- 19) $\text{N} + \text{NO} = \text{N}_2 + \text{O}$
- 20) $\text{N} + \text{O}_2 = \text{NO} + \text{O}$
- 21) $\text{N} + \text{OH} = \text{NO} + \text{H}$

Closing the system of equations given above is produced with the aid of the calorific and thermal equation of states. Calorific equation is written in the following form: $h = \sum_i c_i h_i$, $h_i = \int c_{p_i} dT + h_i^0$, where h_i - enthalpy of components and h_i^0 - the enthalpy of formation. Thermal equation of state is used in the following form:

$$P = \rho RT / \mu, \quad \frac{1}{\mu} = \sum_i c_i / \mu_i,$$

where μ_i - molecular weight of i component. Thus, system of equations consists of two interconnected subsystems: gas-dynamic subsystem and the subsystem for the concentrations which closed with the calorific and thermal equation of states.

In calculations k-w model for turbulent viscosity was used.